Searching for onset of deconfinement via hypernuclei and baryon-strangeness correlations

S. Zhang [a], J.H. Chen [b,*], H. Crawford [c], D. Keane [b], Y.G. Ma [a], Z.B. Xu [d,e]

[a] *Shanghai Institute of Applied Physics, CAS, Shanghai, 201800, China*
[b] *Kent State University, Kent, OH, 44242, USA*
[c] *University of California, Berkeley, CA, 94720, USA*
[d] *Brookhaven National Laboratory, Upton, NY, 11973, USA*
[e] *University of Science and Technology of China, Hefei, Anhui, 230026, China*

A R T I C L E   I N F O

A B S T R A C T

We argue that the ratio $S_3 = {}^3_\Lambda\text{H}/({}^3\text{He} \times \frac{\Lambda}{p})$ is a good representation of the local correlation between baryon number and strangeness, and therefore is a valuable tool to probe the nature of the dense matter created in high energy heavy-ion collisions: quark gluon plasma or hadron gas. A multiphase transport model (AMPT) plus a dynamical coalescence model is used to elucidate our arguments. We find that AMPT with string melting predicts an increase of S_3 with increasing beam energy, and is consistent with experimental data, while AMPT with only hadronic scattering results in a low S_3 throughout the energy range from AGS to RHIC, and fails to describe the experimental data.

Published by Elsevier B.V.

Data from the Relativistic Heavy Ion Collider (RHIC) at Brookhaven National Lab show evidence for partonic collectivity and other likely signatures of quark gluon plasma (QGP) formation during the early stages of the collisions [1–4]. Nevertheless, several important questions remain unresolved, such as the beam energy where the QGP signatures first appear, and other details of the transition between hadronic and deconfined matter. Quantum chromodynamics (QCD) predicts a critical point separating a first-order phase transition and a smooth crossover in the phase diagram of the hot and dense QCD matter [5,6]. It is believed that large fluctuations in phase space population or large correlation length will be one of the experimental signatures of the QCD critical point. Investigations of all of these questions began at the SPS and the upcoming Beam Energy Scan at RHIC [7] will provide an opportunity to study them in more detail. Regardless of how difficult or easy it will be to uncover specific experimental evidence of a critical point, it is a high priority to identify and understand all the observables that offer a prospect of discriminating between hadronic and deconfined matter with good sensitivity.

In calculations from lattice QCD at high temperature, and in models with an ideal quark gas or hadron resonance gas, the cross correlations among the conserved charges show sensitivity to the confined hadron phase or deconfined quark–gluon phase [7–11]. Specifically, in lattice QCD [11], the ratio χ_{11}^{BS}/χ_2^B, the baryon-strangeness correlation (χ_{11}^{BS}) normalized by the baryon–baryon correlation (χ_2^B), approaches unity at high temperature in a deconfined phase, and reaches 0.4 at low temperature in a hadronic phase. The baryon-strangeness correlation coefficient C_{BS} (see Eq. (4)) was argued to be a robust observable to characterize the nature of the system created in high energy heavy-ion collisions: ideal QGP or strongly coupled QGP or hadronic matter [8,9]. Although the local baryon-strangeness correlation is a sensitive probe of the partonic and hadronic phases as predicted by lattice QCD calculation [10], the proposed experimental observable (C_{BS}) is based on global extensive quantities [8,9]. Because it requires a measurement of the global baryon number and strangeness in each event, an experimental analysis based on C_{BS} represents a considerable technical challenge. Further detailed theoretical investigation indicated that a recombination-like hadronization process and hadronic rescattering both have the effect of blurring the fluctuation signal [12,13].

On the other hand, hypernuclei are clusters of nucleons and Λ hyperons [14]. The production of hypernuclei happens through a coalescence mechanism by the overlapping of the wave func-

* Corresponding author.
    E-mail address: jhchen@rcf.rhic.bnl.gov (J.H. Chen).

tions of protons, neutrons and hyperons at the final stage of the collisions [15]. This provides a local correlation of baryons and strangeness on an event-by-event basis [16]. Specifically, the deuteron yield is proportional to the baryon density while triton (t) and helium (^{3}He) are a measure of baryon correlation [17,18]. Similarly, hypertriton production is related to the primordial Λ-p phase space correlation. The ratio $S_3 = {}^3_\Lambda\text{H}/(^3\text{He} \times \frac{\Lambda}{p})$, which we call the Strangeness Population Factor, shows model-dependent evidence of sensitivity to the local correlation strength between baryon number and strangeness, and is demonstrated in this Letter to be a promising tool to study the onset of deconfinement. The ratio S_3 is quantitatively a good representation of χ^{BS}_{11}/χ^B_2 [11] since S_3 contains the local baryon-strangeness correlation in the numerator and the baryon–baryon correlation in the denominator [17]. We expect a prominent enhancement of the Strangeness Population Factor in a system that passes through a deconfined partonic state, relative to what would be observed in a system that always remained in a hadronic phase [8,9].

In this Letter, a multiphase transport model (AMPT) is used to study the effects on S_3 of an existing partonic phase and the subsequent hadronic scattering. The AMPT model is suitable for such studies, since it allows us to switch on and off the string melting mechanism to simulate a partonic phase when the parton density is high at early times, and it also has dynamic transport in the early partonic phase and hadronic scattering at the late stage. The nuclei and hypernuclei are then produced at the final state via Wigner wave-function overlapping of their constituent nucleons and hyperon. If the correlation present at the partonic phase were washed out by the hadronic scattering at the later stage, S_3 would have been similar, regardless of whether the string melting mechanism is on or off in AMPT. In addition, AMPT is also used to compute C_{BS} for a comparison with S_3.

In a thermally equilibrated system, the yields of nuclear clusters via the coalescence mechanism can be related to thermodynamic quantities [19–21]. However, large fluctuations away from thermal equilibrium can result in a locally non-uniform baryon and strangeness correlation on an event-by-event basis [16]. A dynamical coalescence model has been used extensively for describing the production of light clusters in heavy-ion collisions [22] at both intermediate [23–26] and high energies [27–30]. In this model, the clusters are formed in hadron phase-space at freeze out. The probability for producing a cluster is determined by its Wigner phase-space density without taking the binding energies into account. The multiplicity of a M-hadron cluster in a heavy-ion collision is given by

$$N_M = G \int d\mathbf{r}_{i_1} d\mathbf{q}_{i_1} \dots d\mathbf{r}_{i_{M-1}} d\mathbf{q}_{i_{M-1}}$$
$$\times \left\langle \sum_{i_1 > i_2 > \dots > i_M} \rho_i^W (\mathbf{r}_{i_1}, \mathbf{q}_{i_1} \cdots \mathbf{r}_{i_{M-1}}, \mathbf{q}_{i_{M-1}}) \right\rangle. \quad (1)$$

In Eq. (1), $\mathbf{r}_{i_1}, \dots, \mathbf{r}_{i_{M-1}}$ and $\mathbf{q}_{i_1}, \dots, \mathbf{q}_{i_{M-1}}$ are, respectively, the $M-1$ relative coordinates and momenta in the M-hadron rest frame; ρ_i^W is the Wigner phase-space density of the M-hadron cluster, and $\langle \dots \rangle$ denotes the event averaging. G represents the statistical factor for the cluster; it is 1/3 for t, ^{3}He [31] and $^3_\Lambda$H (Λ and $^3_\Lambda$H have the same spin as the neutron and triton, respectively).

To determine the Wigner phase-space densities of ^{3}He and $^3_\Lambda$H, we take their hadron wave functions to be those of a spherical harmonic oscillator [23–26,19,32],

$$\psi = (3/\pi^2 b^4)^{-3/4} \exp\left(-\frac{\rho^2 + \lambda^2}{2b^2}\right), \quad (2)$$

and the Wigner phase-space densities are then given by

$$\rho^W_{^3_\Lambda\text{H}(^3\text{He})} = 8^2 \exp\left(-\frac{\rho^2 + \lambda^2}{b^2}\right) \exp\left(-(\mathbf{k}^2_\rho + \mathbf{k}^2_\lambda)b^2\right). \quad (3)$$

In Eqs. (2) and (3), normal Jacobian coordinates for a three-particle system are introduced as in Refs. [23–26]. (ρ, λ) and $(\mathbf{k}_\rho, \mathbf{k}_\lambda)$ are the relative coordinates and momenta, respectively. The parameter b is determined to be 1.74 fm for ^{3}He [23–26,33] and 5 fm for $^3_\Lambda$H [33] from their rms radii.

The coordinate and momentum space distributions of hadrons (proton, neutron and Λ) at freeze out are obtained from AMPT model calculation [34]. The AMPT model has a good record of agreement with data from RHIC [34], including pion-pair correlations [35] and flow [36]. The model has two modes: the default AMPT model (version 1.11) involves purely hadronic interactions only, while the string melting AMPT (version 2.11) includes a fully partonic stage at the early time of the system evolution. Both modes have been used in the current analysis in order to distinguish the partonic and hadronic effect. The overlap Wigner phase-space density of the three-hadron cluster, $^3_\Lambda\text{H}(p, n, \Lambda)$ and $^3\text{He}(p, p, n)$, is then calculated as discussed above, and a Monte Carlo sampling is employed to determine if the cluster is to form a nucleus or not. A nucleus emerges if the current sample value ρ is less than $\rho^W_{^3_\Lambda\text{H}(^3\text{He})}$. Fig. 1 depicts the $^3_\Lambda$H Wigner phase-space density distribution as a function of (Λ, p) pair momentum at various collision energies in the AMPT model. The coalescence probability is larger in melting AMPT than in the default AMPT model. The difference increases with collision energy.

Fig. 2 shows the S_3 results for minimum-bias Au + Au collisions at various beam energies. The definition of Strangeness Population Factor ($S_3 = {}^3_\Lambda\text{H}/(^3\text{He} \times \frac{\Lambda}{p})$) incorporates the Λ/p ratio in order to remove the absolute difference in Λ and p yields as a function of beam energy. It is interesting to note that S_3 increases with beam energy in a system with partonic interactions (melting AMPT) while it is almost unchanged in a purely hadronic system (default AMPT). The measurement from AGS [33], in spite of large statistical uncertainty, gives the value $\sim 1/3$. The AGS measurement of $S_4 = {}^4_\Lambda\text{H}/(^4\text{He} \times \frac{\Lambda}{p})$ offers further indirect support for the lower value of S_3 at the AGS [33]. A preliminary $^3_\Lambda\text{H}/^3\text{He}$ result for Au + Au collisions at 200 GeV from the STAR Collaboration [37], in combination with the measured Λ/p ratio from the same experiment [38–40], allows us to infer that the measured S_3 at RHIC is consistent with unity within errors. These experimental results are consistent with the melting AMPT calculations and are in contrast to the default AMPT calculations. The data imply that the local correlation strength between baryon number and strangeness is sensitive to the effective number of degrees of freedom of the system created at RHIC, and this number is significantly larger in a system dominated by partonic interactions compared with a pure hadronic gas. The calculated S_3 from melting and default AMPT modes are close at AGS energies and are indistinguishable from the current E864/AGS data. Moving to the top SPS energy and beyond, the calculation using melting AMPT is more than a factor of two larger than the results from default AMPT. It should be noted that if the onset of deconfinement takes place at a specific beam energy, this may result in a sharper increase of S_3 than the AMPT prediction with string melting scenario. Further experimental efforts are eagerly anticipated, including $^3_\Lambda$H measurements as part of the RHIC energy scan.

Furthermore, we investigate the connection between our proposed observable S_3 and the original baryon-strangeness correlation coefficient C_{BS} [8]:
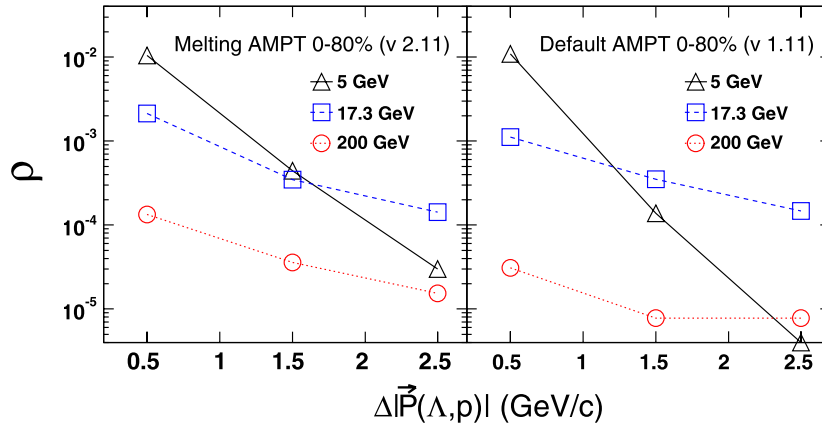
Fig. 1. (Color online.) The Wigner phase-space density ρ for $^{3}_{\Lambda}$H from melting AMPT (left panel) and default AMPT (right panel) as a function of (Λ, p) pair momentum. Densities are shown for $\sqrt{s_{NN}}$ = 5 GeV, 17.3 GeV and 200 GeV. The distributions have been normalized by the number of events at each collision energy.
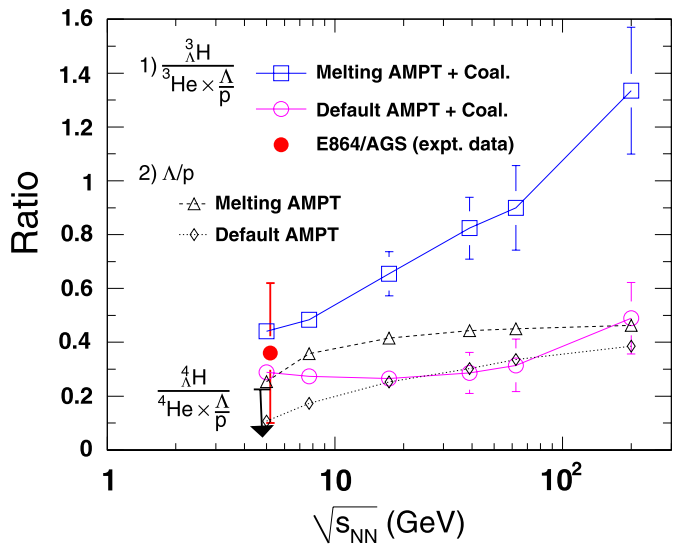

Fig. 2. (Color online.) The S_3 ratio as a function of beam energy in minimum-bias Au + Au collisions from default AMPT (open circles) and melting AMPT (open squares) plus coalescence model calculations. The available data from AGS [33] are plotted for reference. The Λ/p ratios from the model are also plotted.

Fig. 3. (Color online.) The comparison between S_3 and C_{BS} in minimum-bias Au + Au collisions at various beam energies.

$$C_{BS} = -3\frac{\langle BS \rangle - \langle B \rangle \langle S \rangle}{\langle S^2 \rangle - \langle S \rangle^2}, \tag{4}$$

where B and S are the global baryon number and strangeness in a given rapidity window in a given event. As pointed out in Ref. [12], a suitable rapidity window is important to retain the fluctuation signal. We choose the rapidity window of $-0.5 < y < 0.5$ for the present analysis. Fig. 3 shows the C_{BS} in minimum-bias Au + Au collisions as a function of center-of-mass energy from the AMPT model. From top SPS to RHIC energy, the C_{BS} lies between 0.2 and 0.4, and is lower than the expected value of unity for an ideal QGP or $\frac{2}{3}$ for a hadron gas [8]. In addition, we find that the C_{BS} values from melting AMPT and default AMPT are comparable over a wide energy range. As discussed in Ref. [12], the recombination-like hadronization process itself could be responsible for the disappearance of the predicted C_{BS} deconfinement signal. Detailed study indicates that the hadronic rescattering process further blurs the signal [13]. The C_{BS} increases with an increase of the baryon chemical potential μ_B [8] at decreasing beam energy. The Strangeness Population Factor S_3, on the other hand, increases with beam energy in a system involving
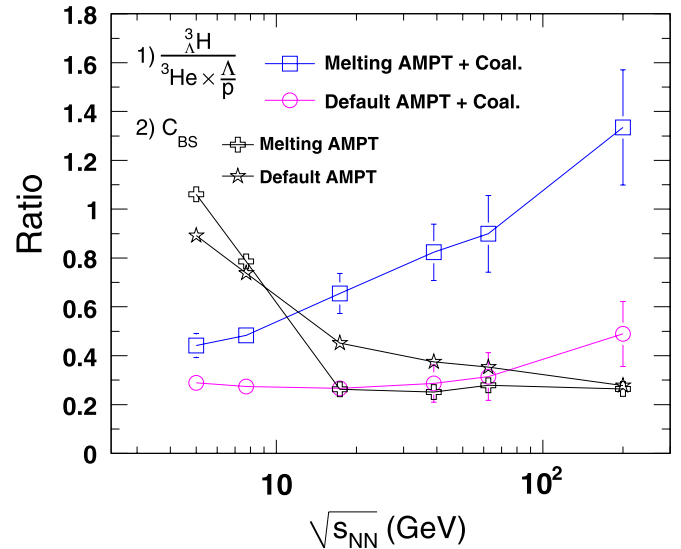
partonic interactions, as shown in Fig. 3. It carries the potential to reliably resolve the number of degrees of freedom of the system created in heavy-ion collisions. This suggests that the global baryon-strangeness correlation coefficient (C_{BS}) is less sensitive to the local baryon-strangeness correlation than the Strangeness Population Factor (S_3) from hypernucleus production. Future precise measurements in comparison with our calculations will provide further insight into these physics questions that are of central importance to relativistic heavy-ion physics.

In summary, we demonstrate that measurements of Strangeness Population Factor S_3 are especially sensitive to the local correlation strength between baryon number and strangeness, and can serve as a viable experimental signal to search for the onset of deconfinement in the forthcoming RHIC Beam Energy Scan.

Acknowledgements

References

[1] I. Arsene, et al., Nucl. Phys. A 757 (2005) 1.
[2] B.B. Back, et al., Nucl. Phys. A 757 (2005) 28.
[3] J. Adams, et al., Nucl. Phys. A 757 (2005) 102.
[4] K. Adcox, et al., Nucl. Phys. A 757 (2005) 184.
[5] Y. Aoki, G. Endrodi, Z. Fodor, S.D. Katz, K.K. Szabo, Nature 443 (2006) 675, and references therein.
[6] F. Karsch, Prog. Theor. Phys. Suppl. 168 (2007) 237.
[7] B.I. Abelev, et al., STAR Note SN0493, http://drupal.star.bnl.gov/STAR/starnotes/public/sn0493.
[8] V. Koch, A. Majumder, J. Randrup, Phys. Rev. Lett. 95 (2005) 182301.
[9] A. Majumder, B. Muller, Phys. Rev. C 74 (2006) 054901.
[10] R.V. Gavai, S. Gupta, Phys. Rev. D 73 (2006) 014004.
[11] M. Cheng, et al., Phys. Rev. D 79 (2009) 074505.
[12] S. Haussler, S. Scherer, M. Bleicher, Phys. Lett. B 660 (2008) 197.
[13] F. Jin, et al., J. Phys. G 35 (2008) 044070.
[14] M. Danysz, J. Pniewski, Phil. Mag. 44 (1953) 348.
[15] H.H. Gutbrod, et al., Phys. Rev. Lett. 37 (1976) 667.
[16] J. Steinheimer, et al., Phys. Lett. B 676 (2009) 126.
[17] H. Sato, K. Yazaki, Phys. Lett. B 98 (1981) 153.
[18] F. Wang, N. Xu, Phys. Rev. C 61 (2000) 021904.

[19] R. Scheibl, U. Heinz, Phys. Rev. C 59 (1999) 1585.
[20] P. Braun-Munzinger, K. Redlich, J. Stachel, in: R.C. Hwa, X.N. Wang (Eds.), Quark Gluon Plasma 3, World Scientific, Singapore, 2004, p. 491, arXiv:nucl-th/0304013.
[21] H. Liu, Z. Xu, arXiv:nucl-ex/0610035.
[22] L.P. Csernai, J.I. Kapusta, Phys. Rep. 131 (1986) 223, and references therein.
[23] M. Gyulassy, K. Frankel, E.A. Relmer, Nucl. Phys. A 402 (1983) 596.
[24] J. Aichelin, A. Rosenhauer, G. Peilert, H. Stöcker, W. Greiner, Phys. Rev. Lett. 58 (1987) 1926.
[25] V. Koch, et al., Phys. Lett. B 241 (1990) 174.
[26] L.W. Chen, C.M. Ko, B.A. Li, Phys. Rev. C 68 (2003) 017601.
[27] J.L. Nagle, Phys. Rev. C 53 (1996) 367.
[28] R. Mattiello, et al., Phys. Rev. C 55 (1997) 1443.
[29] L.W. Chen, C.M. Ko, Phys. Rev. C 73 (2006) 044903.
[30] Y. Oh, C.M. Ko, Phys. Rev. C 76 (2007) 054910.
[31] A. Polleri, et al., Nucl. Phys. A 661 (1999) 452c.
[32] A.T.M. Aerts, C.B. Dover, Phys. Rev. D 28 (1983) 450.
[33] T.A. Armstrong, et al., Phys. Rev. C 70 (2004) 024902.
[34] Z.W. Lin, C.M. Ko, B.A. Li, B. Zhang, S. Pal, Phys. Rev. C 72 (2005) 064901, and references therein.
[35] Z.W. Lin, C.M. Ko, S. Pal, Phys. Rev. Lett. 89 (2002) 152301.
[36] B.I. Abelev, et al., Phys. Rev. Lett. 101 (2008) 252301.
[37] J.H. Chen for the STAR Collaboration, QM09 Proceeding, arXiv:nucl-ex/0907.4147.
[38] B.I. Abelev, et al., Phys. Rev. Lett. 97 (2006) 152301.
[39] J. Adams, et al., Phys. Rev. Lett. 98 (2007) 062301.
[40] B.I. Abelev, et al., Phys. Rev. C 79 (2009) 034909.